npj | science of food

Article

Published in partnership with Beijing Technology and Business University & International Union of Food Science and Technology

https://doi.org/10.1038/s41538-025-00400-3

Protective effects of human breast milk-derived exosomes on inflammatory bowel disease through modulation of immune cells

Ki-Uk Kim[1], Jisu Kim[1], Hyunjun Jang[1], Kang Bin Dan[1], Bo Kyeong Kim[1], Yong Woo Ji[2,3], Dae Yong Yi[4,5] & Hyeyoung Min[1]

Human breast milk (HBM)-derived exosomes play a crucial role not only in infant nutrition but also in modulating inflammation, immunity, and epithelial cell protection. This study investigated how HBM-derived exosomes regulate immune cell development and function. The exosomes promoted the differentiation of naïve $CD4^+$ T cells into Treg and Th2 cells while suppressing their differentiation into Th17 and Th1 cells. They also enhanced the proliferation of intestinal epithelial Caco-2 cells and reduced apoptosis in dextran sulfate sodium (DSS)-damaged caco-2 cells. In a DSS-induced colitis mouse model, the exosomes significantly alleviated disease severity, as evidenced by improvements in colon length, disease activity index, and histology grades. Furthermore, the exosomes normalized $CD4^+$ T cell subsets in the spleen, mesenteric lymph nodes, and colon, restoring levels comparable to controls. These findings suggest that HBM-derived exosomes hold promise as a potential therapeutic strategy for inflammatory bowel disease by modulating T-cell responses and protecting intestinal epithelial cells.

Human breast milk (HBM) plays a vital role in the growth and development of infants. It not only provides essential nutrients but also contains immune-regulatory proteins, hormones, microRNAs, microorganisms, and exosomes[1]. Breastfed children have been reported to experience lower incidences of necrotizing enterocolitis (NEC), gastroenteritis, otitis media, respiratory infections, and acute diseases, as well as reduced rates of obesity, inflammatory bowel disease (IBD), and diabetes[2–4].

Exosomes are nanoscale membrane-bound vesicles originating from endocytic processes and released into the extracellular environment and various bio-fluids[5]. They play a crucial role in promoting the growth and survival of diverse cell types, such as cartilage and endothelial cells, through the modulation of AKT/ERK transcription pathways associated with proliferation[6,7]. Exosomes also significantly influence both innate and adaptive immune responses. For instance, they have been shown to alter the NF-kB inflammatory signaling pathway and impact T-cell priming and activation[8–10]. Recent studies have highlighted the role of extracellular vesicles, including exosomes, in mediating intercellular communication and modulating immune responses[11,12]. Specifically, in the case of HBM, accumulating evidence suggests that HBM-derived exosomes modulate T cells, macrophages, and other immune cell types. They achieve this through the delivery of specific miRNAs, proteins, and lipids that impact gene expression and cellular functions[13,14]. Furthermore, HBM-derived exosomes have been shown to carry immunomodulatory molecules that potentially impact immune tolerance in infants, especially in the development of regulatory T cells and the suppression of pro-inflammatory responses[15]. Recent findings also indicate that exosomes are abundantly present in HBM, with substantial effects on various diseases and immune responses in infants[13,16]

IBD, including ulcerative colitis (UC) and Crohn's disease (CD), is a gastrointestinal (GI) tract disorder characterized by chronic inflammation[17,18]. Symptoms of IBD manifest as chronic diarrhea, abnormal pain, bloody stools, and perianal lesions[17]. Despite extensive research on the causes of IBD, the pathogenesis of both UC and CD remains incompletely understood. Recent studies have shown that a combination of factors, including genetic predisposition, environmental factors, and gut

[1]College of Pharmacy, Chung-Ang University, Seoul, 06974, Republic of Korea. [2]Institute of Vision Research, Department of Ophthalmology, Yonsei University College of Medicine, Seoul, 03722, Republic of Korea. [3]Department of Ophthalmology, Yongin Severance Hospital, Yonsei University College of Medicine, Yongin, 16995, Republic of Korea. [4]Department of Pediatrics, Chung-Ang University Hospital, Seoul, 06973, Republic of Korea. [5]College of Medicine, Chung-Ang University, Seoul, 06972, Republic of Korea. e-mail: hymin@cau.ac.kr

microbiota, may contribute to GI tract disorders, causing epithelial barrier dysfunction and mucosal immune system disruption[19–21]. There is also growing evidence suggesting that intestinal microbiota may play a significant role in IBD development. Abnormal commensal gut bacteria can trigger continuous antigenic stimulation, leading to the activation of a harmful adaptive immune response[20]. As these abnormal bacteria infiltrate intestinal epithelial cells, Th1 and Th17 cells become stimulated and begin to secrete IL-12, IL-23, IL-6, and TNF-α, causing chronic inflammation, tissue damage, and mucosal barrier dysfunction. Consequently, these findings propose that gut microbiota represents a novel etiological factor in IBD[22].

Recent studies have also demonstrated that HBM-derived exosomes contribute to maintaining the integrity of the intestinal epithelial barrier, as indicated by the analysis of tight junction protein expression. Additionally, they have been proven to increase the viability of intestinal cells under oxidative stress[23,24]. Furthermore, using a NEC model mouse, it was confirmed that HBM-derived exosomes reduce the pro-inflammatory cytokine IL-6, thus alleviating intestinal inflammation caused by NEC[25]. These multiple studies have demonstrated that HBM-derived exosomes provide a protective effect in intestinal diseases, with particular emphasis on their role in managing inflammation.

While these studies have highlighted the protective effects of HBM-derived exosomes in intestinal diseases, particularly in managing inflammation, emerging research has begun to uncover their broader immunomodulatory potential[1,13]. Although the beneficial impact of HBM-derived exosomes on the intestine is well-documented, as is their partial influence on immune cells, significant ambiguity remains regarding their specific role in the differentiation of individual T cell subsets. Moreover, the precise mechanisms by which HBM-derived exosomes modulate immune cell development and function in diseases like inflammatory bowel disease (IBD) are still largely unexplored.

This study, therefore, investigates the effects of HBM-derived exosomes on various cell types, including T cells, macrophages, and intestinal epithelial cells, through in vitro experiments. Additionally, it explores their protective effects and influence on immune cell phenotypes and functions using a colitis mouse model. The present findings demonstrate that HBM-derived exosomes possess significant immunomodulatory potential. They not only regulate the polarization and function of T cells but also mitigate inflammatory responses in macrophages. Additionally, the exosomes enhance the proliferation of intestinal epithelial cells and markedly alleviate disease severity in a dextran sodium sulfate (DSS)-induced colitis mouse model. Notably, they increased colon length and restored most CD4 + T cell subsets in the spleen and colon to near-normal levels. These findings underscore the therapeutic potential of HBM-derived exosomes in IBD, particularly through the regulation of T cell development and function and the protection of intestinal epithelial cells from inflammatory damage.

Results

Characteristic of HBM-derived exosome

HBM-derived exosome was isolated using ultracentrifugation and size-exclusion chromatography (SEC) method (Fig. 1A). The presence of exosomal markers, such as CD81, CD9, HSP70, Annexin V, CD54/ICAM-1, Flotillin-1, and Alix, and the cell-specific markers, GM130 confirmed the identity of extracellular vesicles (EVs). Fractions 7–9 exhibited high expression levels of all exosomal specific markers, and thus, these fractions were selected for further study (Fig. 1B). The morphology and size of HBM-derived exosome were determined by transmission electron microscopy (TEM) and nanoparticle tracking analysis (NTA) (Fig. 1C, D), revealing an average size of approximately 53 nm (Fig. 1D).

Cytotoxicity of HBM-derived exosomes in all types of cells

To test the cytotoxicity of HBM-derived exosomes, Annexin V/PI staining and MTT assay were performed. The HBM-derived exosomes were administered to various cell types such as, Raw 264.7 cells, Caco-2 cells, and naïve $CD4^+$ T cells. The HBM-derived exosomes did not exhibit cytotoxicity in naïve $CD4^+$ T cells (Supplementary Fig. 2A). Interestingly, at high doses, they demonstrated a proliferative effect on activated Raw 264.7 cells and Caco-2 cells (Supplementary Fig. 2B, C).

Anti-inflammatory effect of HBM-derived exosomes in Raw 264.7 cells

To investigate the anti-inflammatory effect of HBM-derived exosomes, we measured pro-inflammatory cytokines, including TNF-α, IL-6, and IL-1β, in LPS-activated Raw 264.7 cells. We utilized Western blot and ELISA to assess the expression levels of iNOS, NO, COX-2, PGE_2, and MAPK signaling pathway proteins, such as JNK and ERK. The results revealed a significant reduction in TNF-α expression at a high dose of HBM-derived exosomes, while IL-6 and IL-1β expression levels showed a significant decrease even at a low dose (250 μg/ml) of HBM-derived exosomes (Fig. 2A). Moreover, HBM-derived exosomes decreased the expression level of iNOS and COX-2 in a dose-dependent manner, resulting in a reduction of NO and PGE_2 expression levels (Fig. 2B, C). Furthermore, HBM-derived exosomes inhibited the phosphorylation of MAPK signaling pathway-related proteins, specifically JNK and ERK, leading to the decrease of phospho-JNK (p-JNK) and phospho-ERK (p-ERK).

Effect of HBM-derived exosomes on T cell differentiation

To investigate the effects of exosomes on T cell differentiation, sorted $CD4^+CD25^-CD62L^+CD25^-$ naïve $CD4^+$ T cells were treated with HBM-derived exosomes, and differentiated into various $CD4^+$ T cell subsets. Treatment of naïve $CD4^+$ T cells with a high concentration (1 mg/ml) of HBM-derived exosomes significantly reduced Th17 cell differentiation (Fig. 3A). In contrast, the same highest concentration of HBM-derived exosomes enhanced Treg cell differentiation in naïve $CD4^+$ T cells (Fig. 3B). Moreover, the differentiation of naïve $CD4^+$ T cells into Th1 cells exhibited similar results to Th17 cell differentiation, while Th2 cell differentiation showed a pattern similar to Treg cell differentiation (Fig. 3C, D). To confirm the differentiation of all subsets of $CD4^+$ T cell, transcription factors such as STAT-1, -3, -5, -6, along with their phosphorylated forms, were identified by western blot. Phosphorylation of STAT-1, -3, and -5 was associated with Th1, Th17, and Treg cells, respectively, and was down-regulated by HBM-derived exosomes. Conversely, the activation of STAT6, a transcription factor required for Th2 cell differentiation, was upregulated (Fig. 3E).

Protective effects of HBM-derived exosomes on Caco-2 cells

HBM is absorbed in the intestine through oral intake, making its role in the intestine crucial. Therefore, we examined the effects of HBM-derived exosomes on the proliferation and cell survival of intestinal epithelial Caco-2 cells by treating them with exosomes. Subsequently, we conducted a re-epithelization assay to assess wound healing, and performed western blotting to evaluate the expression of tight junction proteins. The findings revealed that Caco-2 cells treated with a high dose of exosome exhibited an increase in proliferation compared to control cells, indicating a re-epithelialization effect (Fig. 4A). The study also found a significant up-regulation in the expression of tight junction proteins such as ZO-1, OCLD, and CLDN3 following treatment with HBM-derived exosomes (Fig. 4B). Furthermore, we found that pre-treatment of HBM-derived exosomes protected Caco-2 cells from DSS-induced damage by significantly reducing apoptosis in the DSS-treated Caco-2 cells (Fig. 4C).

Alleviation of disease symptoms by HBM-derived exosomes in mouse colitis model

After confirming the beneficial effects of exosomes on macrophages, T cells, and Caco-2 cells, we assessed the disease-alleviating potential of HBM-derived exosomes in acute and chronic mouse colitis models. Parameters such as body weight and DAI scores were monitored to assess the therapeutic impact of exosomes. Interestingly, in both colitis models, there was no significant difference in the body weight between the group treated with DSS alone and the group that received both DSS and exosomes (Figs. 5A, 6A). However, a marked decrease in the DAI scores was observed in the group treated with both DSS and exosomes when compared to the DSS-only

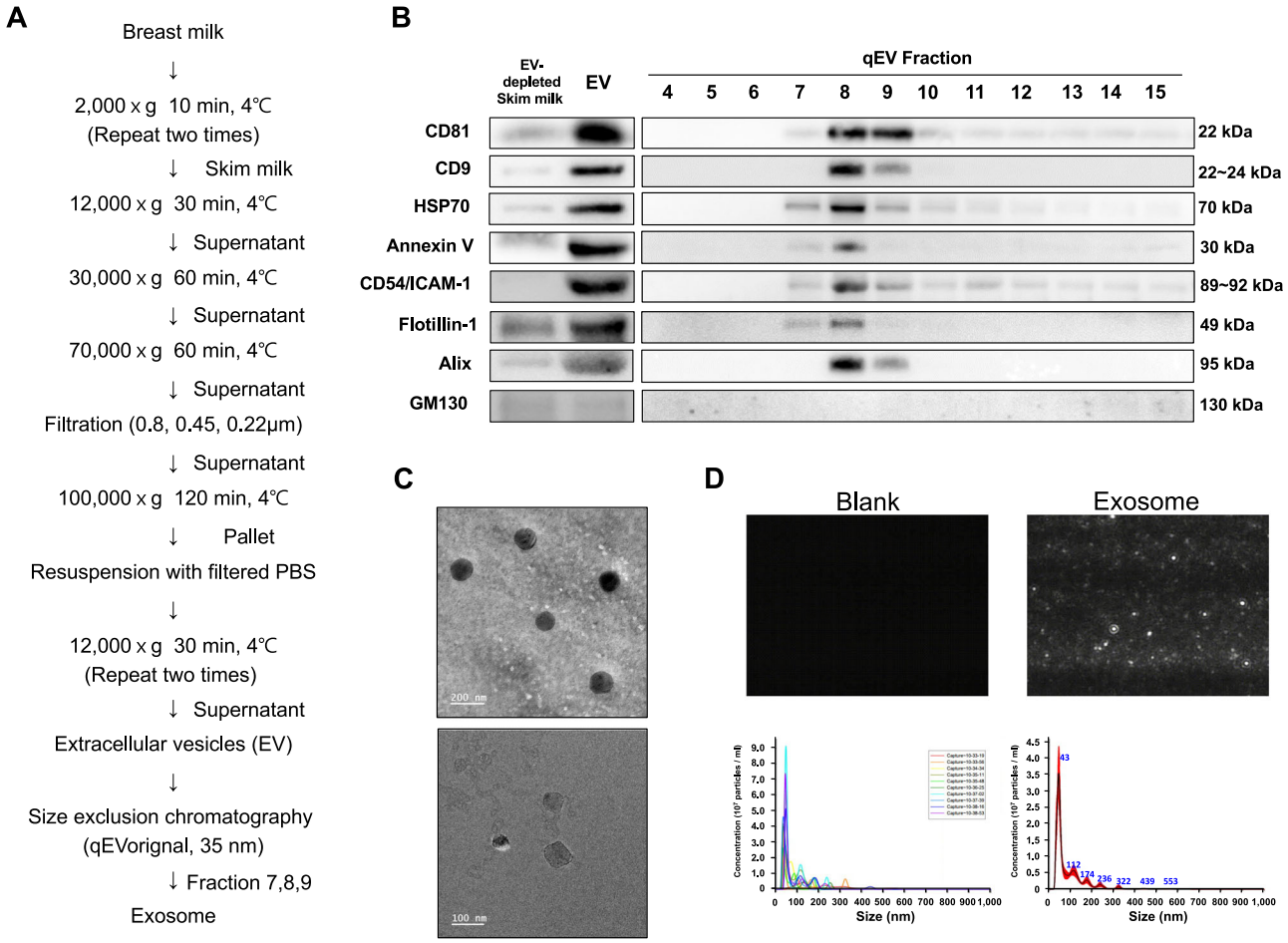

Fig. 1 | Isolation and characterization of human breast milk (HBM)-derived exosome. A Overview of HBM-derived exosome isolation using ultracentrifugation and size-exclusion chromatography (SEC). Samples of HBM were pooled to minimize sample variation ($n = 10$). Initially, 400 mL of HBM was subjected to centrifugation at 2000 × *g*. The upper layer (milk fat) and the pellet (cells and debris) were discarded. The middle portion, known as skim milk, was isolated and utilized for further processing. The final volume of the extracellular vesicle (EV) sample obtained from the skim milk was 3 mL. To sort exosomes, EVs were classified into 15 fractions according to the size by using the SEC (43.92 ± 4.28 μg/μL, $n = 11$). **B** characterization of EVs and exosomes were demonstrated by specific exosome markers, such as CD81, CD9, HSP70, Annexin V, CD54/ICAM-1, Flotillin-1, and Alix, and nonspecific exosome marker, GM130, using western blot. **C, D** Morphology and size were identified by using transmission electron microscopy (TEM; the scale bar is 200 and 100 nm) and nanoparticle tracking analysis (NTA; median of exosome size = 43 nm, the concentration of exosome = 1.39×10^8 particles/mL).

group (Figs. 5B, 6B). Moreover, there was a significant increase in colon length in the group that received exosomes compared to the DSS-only group (Figs. 5C, 6C). Subsequently, we assessed colon histology using Hematoxylin and Eosin (H&E) staining as well as alcian-blue staining. The results revealed that exosome treatment led to a substantial decrease in submucosal layer edema and inflammation due to reduced infiltration of inflammatory cells in the distal colon. Additionally, the findings demonstrated a protective effect of the HBM-derived exosomes on the mucosa and crypts, as evidenced by alcian-blue staining, which specifically targets and stains these areas (Fig. 7).

Immunomodulatory effect of HBM-derived exosome in a mouse colitis model

To understand the immunomodulatory potential of HBM-derived exosomes, the composition of immune cells in the colon, MLN, and spleen was assessed by immunohistochemistry and flow cytometry. We found that the infiltration of macrophages and T cells in the colon was significantly decreased in both the acute and chronic models following exosome treatment (Fig. 7). Flow cytometry analysis showed that the frequency of macrophages was decreased in the MLN, while that of TFG-β-producing macrophages was increased in the spleen and MLN of exosome-treated mice in the acute model (Fig. 5). In addition, in the acute model, exosome treatment significantly reduced Th17 in the spleen, MLN, and colon, as well as Th1 cells in the MLN and colon (Fig. 5). In the chronic model, the exosome treatment effectively reduced the frequency of Th17 and Th1 cells in all examined organs, while increasing Treg and Th2 cells (Fig. 6).

Discussion

Exosomes are nano-sized vesicles secreted by cells, containing bioactive molecules such as proteins and nucleic acids[13]. They play a critical role in intercellular communication, and their role in health and disease is an active area of research[26]. Recent studies have specifically focused on exosomes derived from HBM and their potential therapeutic benefits[13,27,28]. HBM-derived exosomes have been found to possess beneficial physiological characteristics, including anti-inflammatory properties and the ability to modulate immune responses[13,29,30]. As a result, researchers anticipate significant therapeutic benefits in the management of intestinal diseases through the use of HBM-derived exosomes, leading to numerous ongoing research initiatives[23–25]. Although several studies have established the production of immune-related cytokines, such as IFN-γ, IL-5, -9, -10, and -13, in connection with HBM-derived exosomes, their specific influence on the immune system, encompassing both innate and adaptive immunity, remains less explored. Further in vivo studies and clinical trials are required to confirm these beneficial effects in a disease model. Therefore, this study

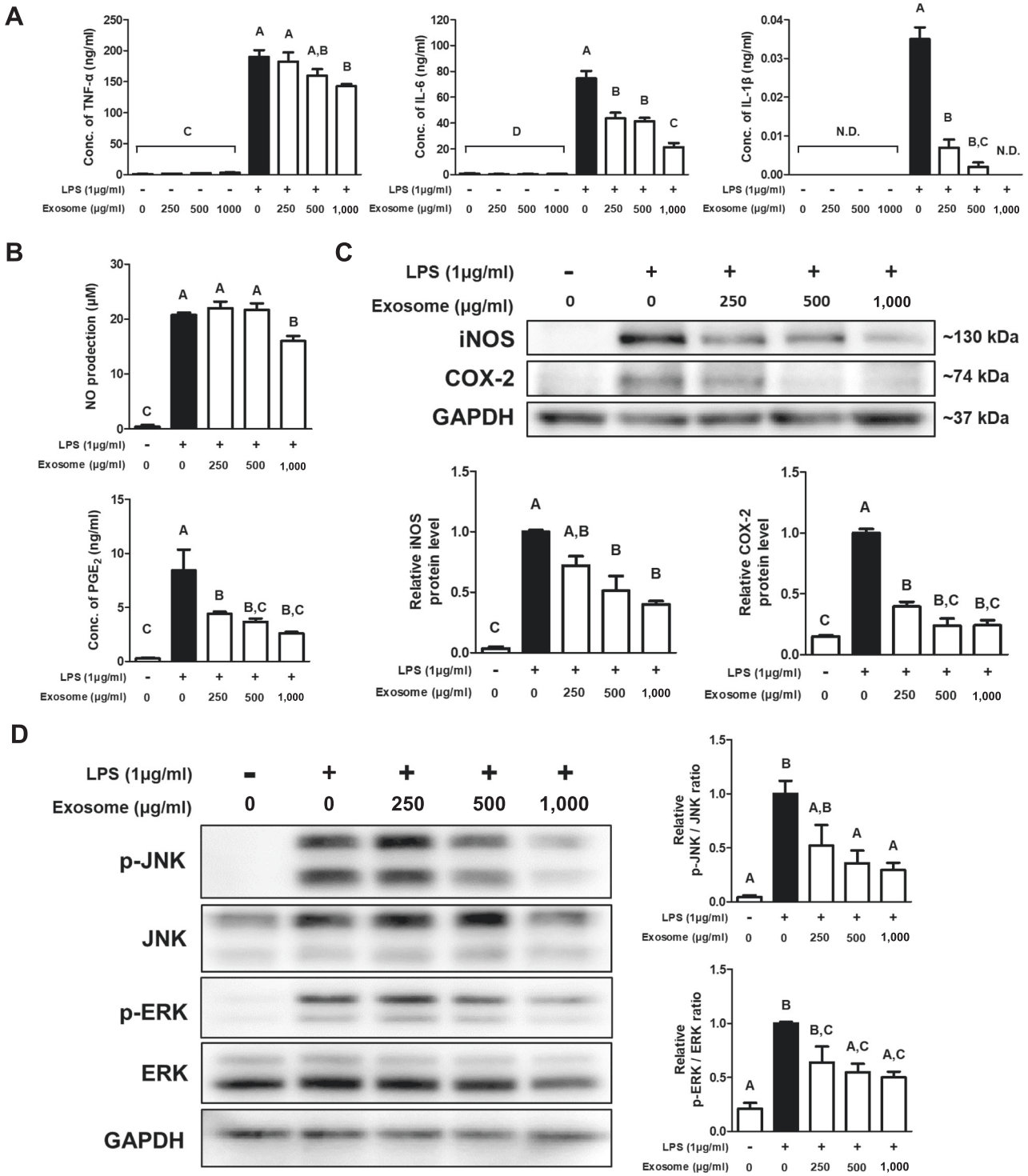

Fig. 2 | Anti-inflammatory effects of HBM-derived exosomes on RAW 264.7 cells. **A**–**C** Raw 264.7 cells were treated with HBM-derived exosomes for 24 h and activated with LPS for 20 h. **A**, **B** Cultured media were harvested, and expression levels of pro-inflammatory cytokines (TNF-α, IL-6, IL-1β) and other mediators (NO and PGE_2) were measured using ELISA and NO assay. **C** Total protein was extracted from cells. Protein expression of iNOS and COX-2 was demonstrated by western blot. **D** Raw 264.7 cells were treated with HBM-derived exosomes for 24 h and activated with LPS for 15 min. Phosphorylation of JNK and ERK was identified by western blot. Data represent the means ± SEM ($n \geq 3$). The significance of the data were examined by one-way ANOVA with Tukey's post hoc test ($P < 0.05$).

emphasizes the potential immunomodulatory and anti-inflammatory functions of HBM-derived exosomes, and applies them to an IBD model to confirm their functions.

In this study, we isolated exosomes using a qEV size-exclusion chromatography column, a method that is widely recognized for yielding high-purity exosome fractions while minimizing contamination from other extracellular vesicles and nanovesicles. Although the measured size of the isolated vesicles peaks at 43 nm, which is smaller than the typical exosome size, this does not imply the presence of exomeres. According to a recent study, the centrifugal force applied in our protocol is lower than the threshold required for exomeres isolation, supporting that our particles are indeed exosomes[31]. Additionally, exomeres lack the specific exosomal

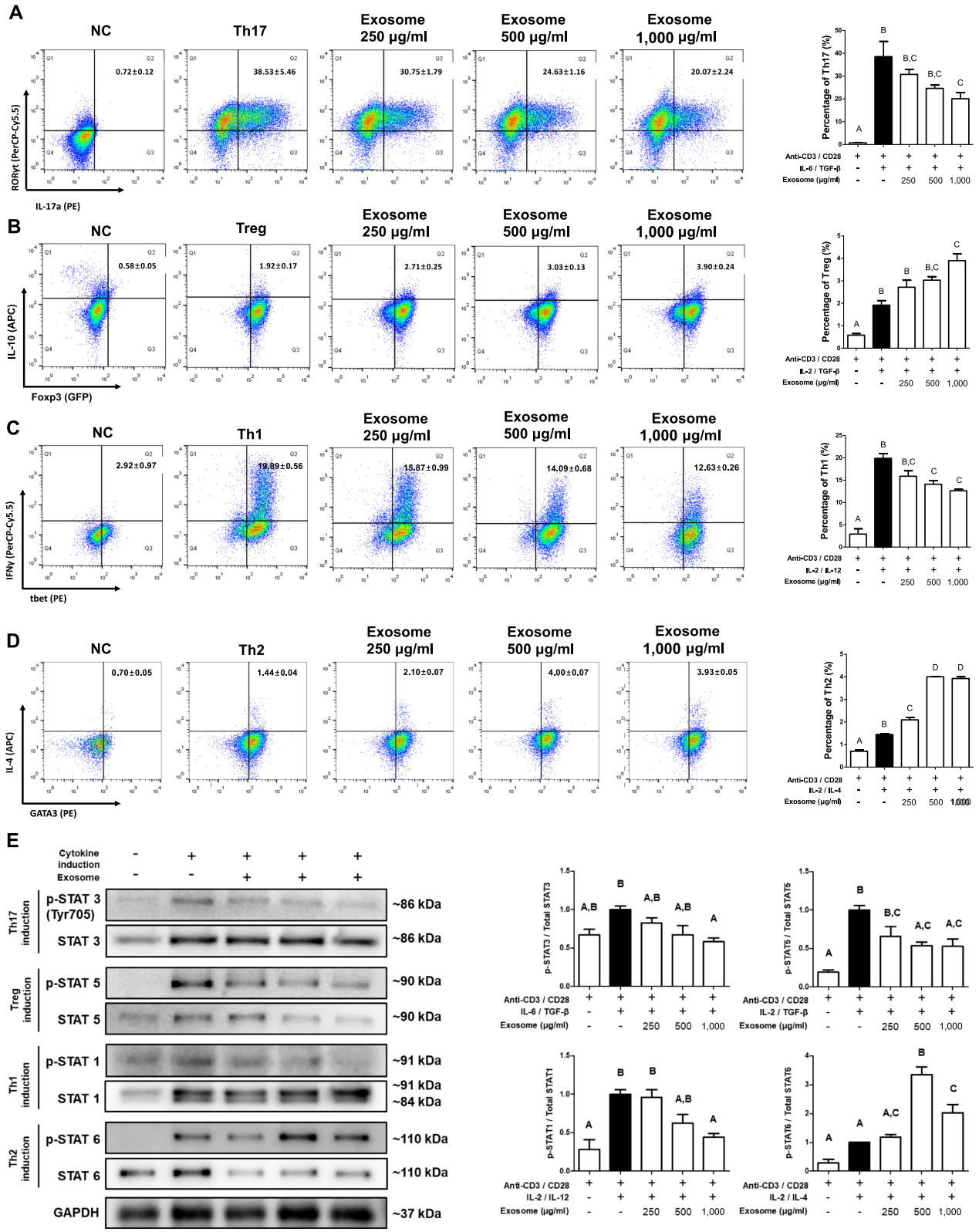

Fig. 3 | Effect of HBM-derived exosomes on the differentiation of naïve CD4$^+$ T cells. A–D Naïve CD4$^+$ T cells were treated with the HBM-derived exosomes and differentiated into Th1, Th2, Th17, and Treg cells. Different cytokines (Th17: IL-17a, Treg: IL-10, Th1: IFN-γ, Th2: IL-4) and specific intracellular markers (Th17: RORγt, Treg: Foxp3, Th1: t-bet, Th2: GATA-3) were observed by Flow cytometry. **E** Total protein was extracted from each differentiated CD4$^+$ T cell, and transcription factors (Th17: STAT3 and p-STAT3, Treg: STAT5 and p-STAT5, Th1: STAT1 and p-STAT1, Th2: STAT6 and p-STAT6) were demonstrated by western blot. Data represent the means ± SEM ($n \geq 3$). The significance of the data were examined by one-way ANOVA with Tukey's post hoc test ($P < 0.05$).

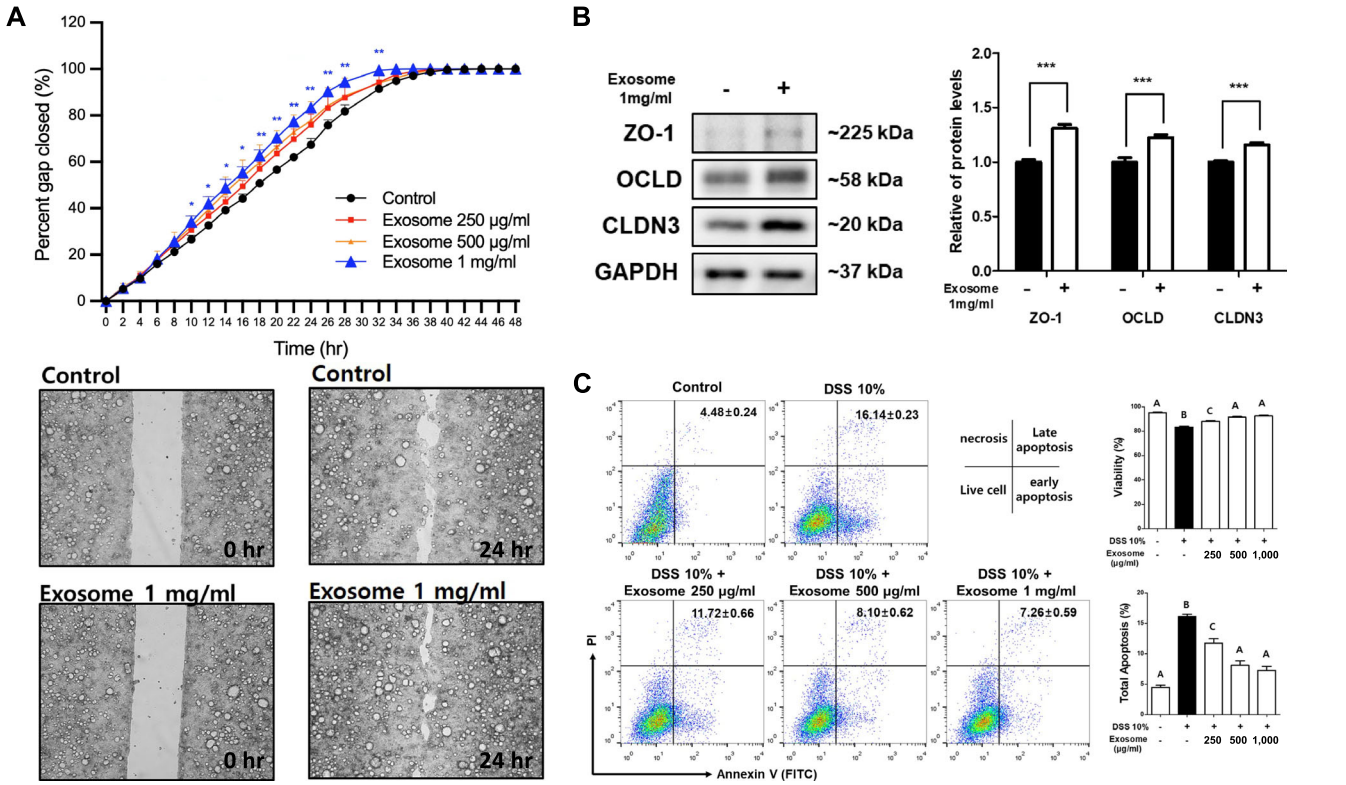

Fig. 4 | Effects of HBM-derived exosomes on Caco-2 cells. A The wound closed values were indicated by measuring the percentage of gap closed compared with the 0 h point for each sample. The percent gap closed was shown in a dose- and time-dependent manner as a graph. Microscopic images were captured using a JuLI Stage Real-Time Cell History Recorder at the indicated time points. **B** Caco-2 cells were treated with the HBM-derived exosomes (1 mg/mL), and total protein was extracted. Protein expression of tight junction proteins (ZO-1, OCLD, CLDN3) were measured by western blot. **C** Caco-2 cells were pretreated with HBM-derived exosomes for 1 day and damaged for 1 day using DSS. Annexin V/PI staining was used to measure the apoptosis and viability. Data represent the means ± SEM (n ≥ 3). The significance of the data were examined by one-way ANOVA with Tukey's post hoc test. $^{*}P < 0.05$; $^{**}P < 0.01$; $^{***}P < 0.001$; $^{****}P < 0.0001$.

markers CD81 and CD9, both of which are present in our isolated vesicles, further confirming their identity as exosomes[32].

Previous research has demonstrated the anti-inflammatory properties of milk-derived exosomes[25,33,34]. Consistent with these findings, the present study observed that exosomes from HBM reduced the production of TNF-α, IL-6, and IL-1β (Fig. 2A). Furthermore, the results indicated that HBM-derived exosomes decreased iNOS, NO, COX-2, and PGE_2 levels (Fig. 2B, C). Inflammatory signaling pathways, including NF-kB and MAPK pathway, play significant roles in inflammation[35,36]. Porcine milk-derived exosomes were found to protect the intestine from LPS-induced injury by reducing inflammation, and this protective effect resulted from the inhibition of the NF-κB and p53 pathways[37]. In addition to the NF-κB pathway, the present study discovered that HBM-derived exosomes were associated with the MAPK pathway and led to the reduction of MAPK signaling, including the activation of ERK and JNK, which contributed to their anti-inflammatory effects (Fig. 2D). These finding suggested that the milk-derived exosomes may have an anti-inflammation effect though controlling the NF-κB and MAPK pathway in various diseases.

The present study also emphases on exploring the potential role of HBM-derived exosomes in the differentiation of naïve $CD4^+$ T cells, aiming to investigate their positive impact on immunity. The results demonstrated that exosomes led to a decrease in $RORgt^+IL\text{-}17a^+$ levels and an increase in Foxp3 expression. This, in turn, diminished Th17 cell differentiation while promoting Treg cell differentiation (Fig. 3A, B). These findings align with previous studies that have shown treatment of arthritis mice with high levels of bovine milk-derived EV resulting in increased expression of GATA-3 (Th2) and Foxp3 (Treg)[38]. Furthermore, HBM-derived exosomes suppressed the production of IL-2, IFN-γ, and TNF-α in PBMCs when induced by CD3, while simultaneously boosting the population of $FoxP3^+CD4^+CD25^+$ regulatory T cells within PBMCs[13]. Additionally, these exosomes influenced the levels of $t\text{-}bet^+IFN\text{-}\gamma^+$ and $GATA3^+IL\text{-}4^+$, resulting in a decrease in Th1 cell differentiation and an increase in Th2 cell differentiation (Fig. 3C, D). Moreover, to provide further evidence for the differentiation potential of HBM-derived exosomes, we assessed the activation of the STAT family, which are signal transducers and activators of transcription associated with JAK-STAT signaling. This signaling pathway plays a crucial role in regulating T cell metabolism by directly impacting metabolism-related gene expression and indirectly affecting upstream or regulatory factors, ensuring the adaptation of T cell metabolism to various demands and conditions[39]. Specifically, STAT6, STAT3, and STAT1 are transcription factors that are related to IL-4, IL-17, and IFN-γ, respectively[40–42]. In line with this, the present study corroborated previous research by showing that an increase in IL-4 was accompanied by an elevation in STAT6 activation. Additionally, a decrease in IL-17 and IFN-γ was observed, which was associated with diminished activation of STAT3 and STAT1 following treatment with these exosomes (Fig. 3E). However, we noticed a divergent pattern when it came to the activation of STAT5, a transcription factor linked to Treg cells, compared to the level of Treg differentiation (Fig. 3D, E). This indicates that clarifying the effects of HBM-derived exosomes on Treg cells remains a contentious issue. Nevertheless, given their immunomodulatory effects, it is expected that HBM-derived exosomes may still play a crucial role in modulating the immune system during infancy.

Human breast milk-derived exosomes have been shown to protect intestinal barriers, mitigate oxidative stress, and exert anti-inflammatory effects in mouse models of necrotizing enterocolitis (NEC)[23–25,43]. Furthermore, preterm human breast milk exosomes enhance epithelial cell proliferation and migration, preserve ileal villous integrity, and restore enterocyte proliferation in NEC models, highlighting their role in promoting cell growth and regulating inflammation[44]. These findings suggest

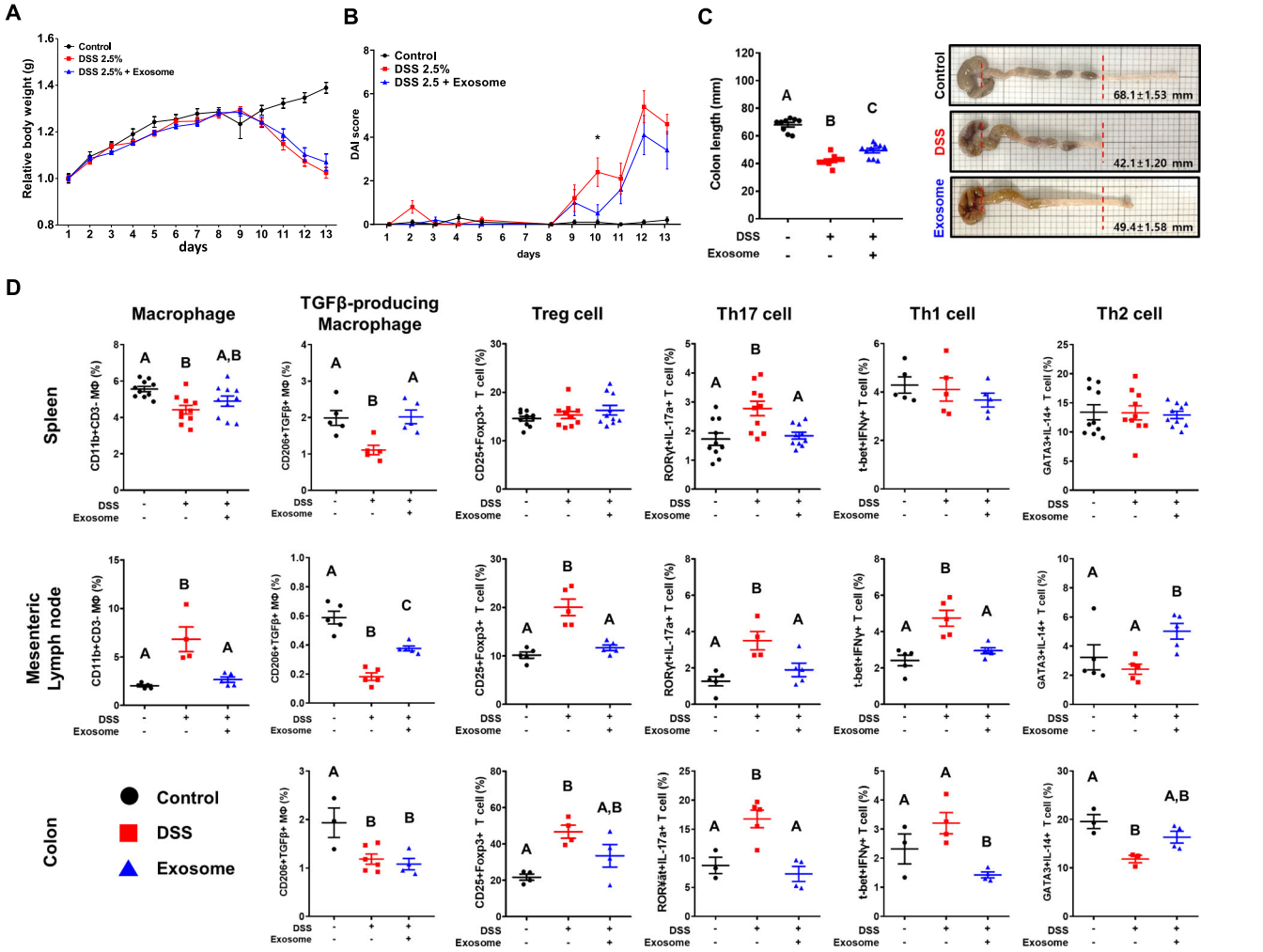

Fig. 5 | Therapeutic effects of HBM-derived exosomes in acute DSS-induced colitis. HBM-derived exosomes were orally administrated to mice with acute DSS-induced colitis. **A–C** Various parameters such as body weight, disease activity index (DAI) score, and colon length were measured. **D** Diverse immune cells, including macrophages, regulatory T cells (Treg cells), Th17 cells, Th1 cells, and Th2 cells, was analyzed in different organs, including the spleen, mesenteric lymph nodes, and colon. Flow cytometry was used as the method to quantify these immune cell populations. Significance of the data were examined by one-way ANOVA with Tukey's post hoc test. Control ($n = 10$), DSS group ($n = 10$), DSS + exosome group ($n = 10$). Data were presented as mean ± SEM (for A, B) and as individual samples represented by dots with mean values shown as bars (for **C**, **D**). $^*P < 0.05$.

that HBM exosomes have the potential to protect and repair the intestinal epithelium, which is often damaged in IBD. To confirm these effects, we conducted experiments using Caco-2 cells and acute and chronic mouse colitis models. The results showed that HBM-derived exosomes enhanced cell viability and wound healing in damaged Caca-2 cells, while reducing apoptosis (Fig. 4). In addition, we observed the up-regulation of tight junction proteins such as ZO-1, OCLD, and CLDN3 upon exosome treatment. Consistent with these findings, Chiba et al. reported that ZO-1 expression in Caco-2 cells is induced by the suppression of REDD1, a stress-induced regulator, and by an increase in mTOR phosphorylation following HBM exosome treatment[45]. Moreover, exosome treatment enhanced AMPK phosphorylation and GLP-2 secretion, which together promoted the expression of ZO-1, OCLD, and CLDN1, and strengthened the intestinal barrier[23,46]. While the use of only a single cell line (Caco-2) may inherently limit the extrapolation of these findings to other epithelial cell types, the observed outcomes underscore the beneficial effects of HBM-derived exosomes on intestinal barrier function.

In DSS-induced mouse colitis models, exosome treatment not only increased colon length and reduced DAI score but also improved epithelial integrity accompanied by a decrease in pronounced edema in the submucosal layers (Fig. 7). The results strongly indicate that the exosomes might contribute to maintaining the integrity of the intestinal barrier, which is crucial in preventing the exacerbation of IBD, and they support the potential therapeutic role of HBM-derived exosomes in managing intestinal diseases.

In addition, we also evaluated the immunomodulatory effects of HBM-derived exosomes in the mouse colitis model. Macrophage infiltration leads to the development of intestinal inflammation and the secretion of pro-inflammatory cytokines and bioactive substances that actively participate in the inflammatory response. Concurrently, infiltration of immune cell such as Th17 cells and $CD4^+$ T cells contribute to colon tissue damage, inflammation, and intestinal mucosal inflammation in UC[47,48]. In this study, we observed that the administration of HBM-derived exosomes can potentially alleviate intestinal inflammation by reducing the infiltration of macrophages and T cells in the colon (Fig. 7). Moreover, HBM-derived exosomes demonstrated the ability to down-regulate Th17 cells, known for primarily secreting the pro-inflammatory IL-17a and playing a significant role in inflammatory diseases. Additionally, the exosomes also down-regulated Th1 cells, which are conventional mediators of CD, in both acute and chronic models (Figs. 5D, 6D)[49,50]. Conversely, Treg cells, crucial in reducing immune activation and preventing systemic autoimmunity, were found to be upregulated in the chronic model following administration of

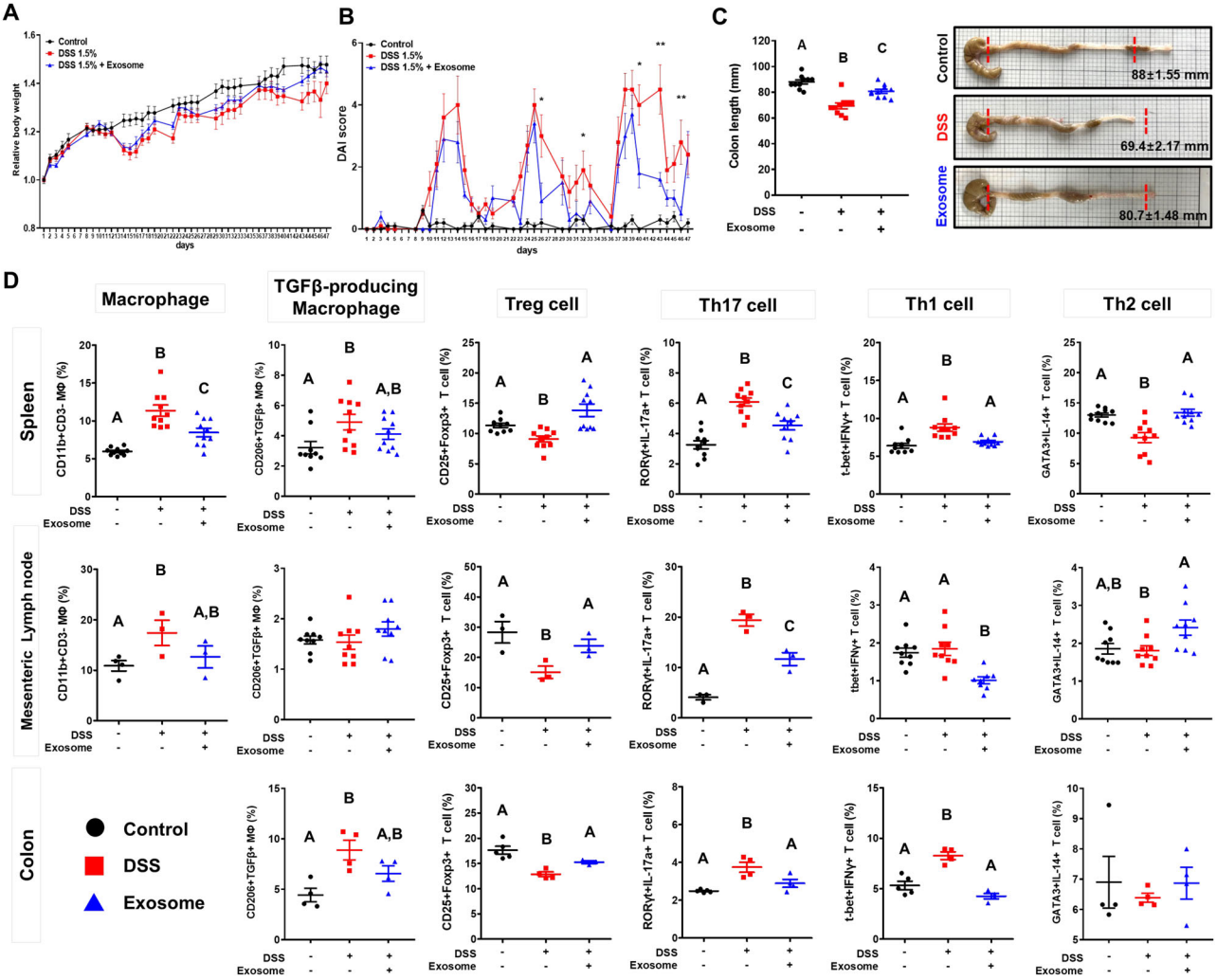

Fig. 6 | Therapeutic effects of HBM-derived exosomes in chronic DSS-induced colitis. HBM-derived exosomes were orally administrated to mice with chronic DSS-induced colitis **A**–**C** Various parameters such as body weight, disease activity index (DAI) score, and colon length were measured. **D** Diverse immune cells (macrophage, Treg cell, Th17 cell, Th1 cell, and Th2 cell) in different organs (spleen, mesenteric lymph node, and colon) were measured by flow cytometry. Significance of the data were examined by one-way ANOVA with Tukey's post hoc test. Control ($n = 10$), DSS group ($n = 10$), DSS + exosome group ($n = 10$). Data were presented as mean ± SEM (for **A**, **B**) and as individual samples represented by dots with mean values shown as bars (for **C**, **D**). $^{*}P < 0.05$; $^{**}P < 0.01$.

HBM-derived exosomes. Similarly, Th2 cells, playing a key role in maintaining mucosal homeostasis and providing protection against pro-inflammatory pathways in chronic intestinal inflammatory disorders such as IBD, were also upregulated in the chronic model following exosome treatment (Fig. 6D)[51,52]. These findings suggest that HBM-derived exosomes have the potential to modulate the balance of different T cell subsets, highlighting their potential role in immunomodulation.

In summary, this study unveils the immunomodulatory and anti-inflammatory properties of HBM-derived exosomes. Our findings demonstrate that these exosomes actively shape the differentiation trajectory of naïve $CD4^{+}$ T cells, enhancing the development of Tregs and Th2 subsets, while suppressing pro-inflammatory Th1 and Th17 lineages. Moreover, HBM-derived exosomes attenuated the production of pro-inflammatory cytokines and inflammatory mediators in macrophages, underscoring their potential to modulate immune responses at multiple levels. These results position milk-derived exosomes as promising candidates for therapeutic intervention in intestinal pathologies, particularly IBD, with broader implications for immune regulation and inflammation control in diverse disease contexts. Collectively, our study suggests that HBM-derived exosomes may hold substantial therapeutic value in harnessing and regulating immune function across a spectrum of inflammatory disorders.

Despite these promising findings, several critical limitations deserve attention. First, the regulation of cell proliferation and apoptosis is highly specific to each cell type, requiring cautious interpretation of our results across varied cellular settings. Additionally, IBD includes at least two distinct and intensely inflammatory autoimmune pathways, presenting a complex, multifactorial disease environment that may react differently to HBM-derived exosome exposure. To ensure the safety of HBM exosomes, standard genotoxicity testing in normal, healthy gut mucosal cells should be conducted in future in vitro and clinical studies. Furthermore, subsequent research should systematically explore alternative therapeutic approaches, such as the influence of prebiotics on microbiome modulation across various IBD subtypes and diverse life stages with distinct physiological characteristics.

Although we increased the sample size and pooled samples to reflect the diversity of HBM-derived exosomes, it is essential to recognize that these exosomes inherently exhibit variability due to maternal environmental, xenobiotic, and genetic factors[53,54]. Specific genetic mutations and environmental exposures may alter gene expression profiles and immune-modulatory capabilities within exosomes[54,55], and polymorphisms associated with environmental and xenobiotic factors could also alter the therapeutic outcomes of exosomes. For example, Miklavcic et al. reported that single-nucleotide

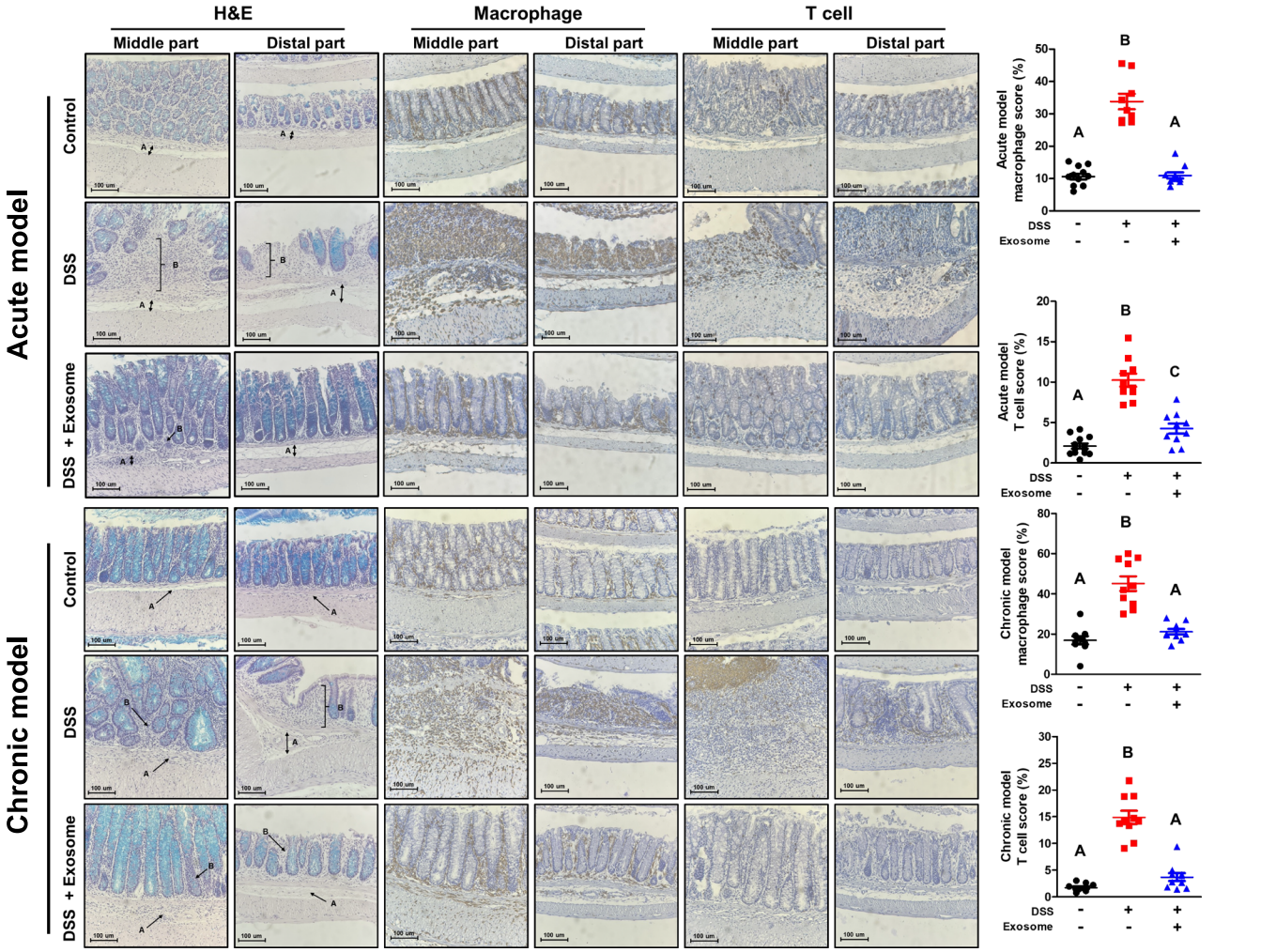

Fig. 7 | The histology of the colon in mice with DSS-induced colitis upon exosome treatment. Hematoxylin & eosin staining and immunohistochemistry was performed to identify the morphological changes in the colon and to detect the infiltration of macrophages and T cells. Significance of the data were examined by one-way ANOVA with Tukey's post hoc test ($P < 0.05$). The scale bar is 100 μm. **A**: extensive edema of the submucosal layer, **B**: inflammatory cell infiltration. Samples of all groups ($n = 10$).

polymorphisms (SNPs) in the FADS gene locus (rs174546 and rs174575) change the composition of polyunsaturated fatty acid in human milk EVs, which are important to EV bioavailability, including passage across epithelial and endothelial barriers[56]. Furthermore, the microbiome, particularly its interaction with genetic and epigenetic factors such as microRNAs which are abundant within milk exosomes, may significantly influence both the safety and effects of HBM-derived exosomes. It is already well established that both the microbiome and exosomal microRNAs mediate various physiological functions of breast milk, suggesting that the interplay between these factors could have a profound effect[57]. Given that the various host factors can influence exosome functionality, an integrated approach that considers the complexity of the relationship between these factors should be explored to better understand how they impact the safety, functionality,y and therapeutic potential of HBM-derived exosomes.

Methods

Collection of breast milk samples

HBM samples were supplied at Chung-Ang University Breastfeeding Research institute (Seoul, Korea) from recent lactating mothers who agreed to analysis their HBM. HBM samples were provided in a fresh state and aliquoted (15 mL) and stored immediately at −80 °C until experiment was conducted.

Isolation of breast milk-derived exosome

HBM samples were thawed and pooled at least 30 to reduce the variability between the samples. HBM-derived exosomes were sequentially isolated by the ultracentrifugation and size-exclusion chromatography (SEC) method. First, the 500 mL of HBM samples were centrifuged two times at 2000 × *g* for 10 min at 4 °C. As a result, they were separated into three parts (fat, whey, cell and debris), and skim milk was only used for the next step. Skim milk was centrifuged at 12,000 × *g* for 10 min at 4 °C, and the supernatants were transferred to Optiseal tubes (Beckman Coulter, Brea, CA, USA) which can successfully withstand the ultracentrifugation steps. The supernatants were successively ultra-centrifuged at 30,000 × *g* (60 min) and 70,000 × *g* (60 min) at 4 °C (Beckman Coulter Optima XE-100 with Type 50.2 Ti Fixed angle ultracentrifuge rotor). Then the supernatants were sequentially filtered through 0.8-, 0.45-, 0.22-μm syringe filters (Satorius AG, Göttingen, Germany). Filtrates were centrifuged at 100,000 × *g* for 120 min at 4 °C, and a brown clear pellet, which is EV, can be detected. Then, the pellets of EVs were resuspended in 2 mL autoclaved PBS and loaded on a qEV column 35 nm (Izon Science Ltd, New Zealand) following the manufacturer's instructions. A total of 16 fractions were extracted and used for further study.

Nanoparticle tracking analysis (NTA)

Nanoparticle tracking analysis was performed using a NanoSight NS300 (Malvern Panalytical Ltd., Malvern, UK) and NTA 3.4 software build 3.4.4

(Malvern Panalytical Ltd.). The sample eluted from SEC was diluted 1:20 in deionized water, and the final volume of 0.6 ml was used for the analysis. The exosomes were analyzed in flow mode with a syringe pump speed of 30. Each measurement was recorded ten times for 30 s using a 488 nm laser and a built-in sCMOS camera. The camera level was set to 11 to visually distinguish each exosome. Additional measurement conditions included a detection threshold of 5, cell temperature of 25 °C, and viscosity of Water (0.871–0.872 cP).

Transmission electron microscopy (TEM)

Fractions 7–9 of HBM-derived exosome were used for analysis and diluted 1:1000 with PBS. About 10 uL of diluted exosome were layered on Formvar/Carbon films on a 400 mesh copper grid for 15 min. The grids were rinsed with deionized distilled water and finally air-dried at RT for 1 week. The morphology of exosomes was observed by JEM-F200 (20 kV, JEOL Ltd, Tokyo, Japan).

Raw 264.7 cell and Caco-2 cell culture

Raw 264.7 cells (mouse macrophage cell line) and Caco-2 cells (human colon epithelial cell line), which were purchased from the Korea Cell Line Bank (Seoul, Korea), were maintained in Dulbecco's Modified Eagle's Medium (DMEM; Welgene, Daegu-si, Korea) containing 10% (v/v) fetal bovine serum (FBS; Welgene) and 1% (v/v) penicillin/streptomycin (P/S; Gibco, Grand Island, NY, USA) at 37 °C.

Isolation of naïve $CD4^+$ T cells

Four-week-old male C57BL-6 mice, which were purchased from Raonbio (Seoul, Korea) and $Foxp3^{GFP+}$ transgenic (TG) mice, which were kindly provided by Prof. K. W. Hwang (Chung-Ang University, Seoul, Korea), were used. Spleen were isolated from mice, and splenic lymphocytes were harvested after the treatment of red blood cell lysis. The cells were washed with PBS and resuspended in MACS buffer. $CD4^+$ T cells were positively selected by anti-CD4 microbeads and magnetic MidiMACS Separator (Miltenyi Biotec, Bergisch Gladbach, Germany). Total $CD4^+$ T cells, which were positively harvested by anti-CD4 microbeads, were stained with FITC -conjugated anti-human/mouse CD44 antibody (clone IM7, Biolegend, San Diego, CA, USA), PE-conjugated anti-human/mouse CD25 antibody (clone PC61, Biolegend), PE-cyanine5-conjugated anti-mouse CD62L antibody (clone MEL-14, eBioscience, San Diego, CA, USA), PE-cyanine7-conjugated anti-mouse/human CD44 antibody (clone IM7, Biolegend), and APC-conjugated anti-mouse CD4 antibody (clone RM4-5, Biolegend) to sort $CD4^+CD25^-CD62L^+CD25^-$ or $CD4^+CD25^-CD62L^+CD25^-Foxp3^-$ naïve $CD4^+$ T cells by BD FACS Aria II cell sorter (BD Biosciences, Franklin Lakes, NJ, USA) (Supplementary Fig. 1). The naïve $CD4^+$ T cells were cultured in RPMI1640 complete medium supplemented 10% (v/v) FBS (Welgene), 1% (v/v) P/S (Gibco), L-glutamine (Corning, Corning, NY, USA), MEM non-essential amino acids (Corning), HEPES (Corning), sodium pyruvate (Corning), and 2-mercaptoethanol (Sigma-Aldrich, St. Louis, MO, USA) at 37 °C in 5% CO_2.

Cytotoxicity and apoptosis test of human breast milk-derived exosome in several types of cell

HBM-derived exosomes were determined for cytotoxicity through 3-(4, 5-dimethylthiazol-2-yl)-2,5-diphenyltetrazolium bromide (MTT) assay. Briefly, Raw 264.7 cells were seeded at a density of 3×10^4 cells with 100 µL cell culture medium in a 96-well plate. Raw 264.7 cells were stimulated with 1 µg/mL of LPS (Sigma-Aldrich, St. Louis, MO, USA) for 18 h. On the other hand, Caco-2 cells were seeded at a density of 2×10^4 cells in 100 µL of cell culture medium per well in a 96-well plate. Then, HBM-derived exosomes were treated in dose-dependent manners (250, 500, 1000 µg/mL) at 37 °C for 24 h. About 10 µL of MTT (5 mg/mL) was treated in each well for 4 h and 100 µL of 0.04 N HCl in isopropanol was added. Finally, the absorbance was determined at 540 nm to identify live cells using an EMax® microplate reader (Molecular Devices, Sunnyvale, CA, USA). Furthermore, Caco-2 cells were seeded in a 24-well plate at a density of 2×10^5 cells per well, using 500 µL of cell culture medium. Subsequently, HBM-derived exosomes were treated in the cells in a dose-dependent manner, with concentrations of 250, 500, and 1000 µg/ml. The cells were then incubated at 37 °C for 24 h. After the incubation period, the Caco-2 cells were induced to undergo apoptosis by treating them with 10% DSS for an additional 24 h. Following this, the cells were collected and rinsed with Annexin V binding buffer (Invitrogen, Carlsbad, CA, USA). In the case of naïve $CD4^+$ T cells were seeded at a density of 4×10^5 cells per well in a 24-well plate with 250 µL of RPMI1640 complete medium and cultured with HBM-derived exosomes in a dose-dependent manner (31.25, 62.6, 125, 250, 500, 1000 µg/mL) at 37 °C for 24 h. The cells were collected and washed by Annexin V binding buffer (Invitrogen). To evaluate the apoptosis of HBM-derived exosome, FITC-conjugated Annexin V and propidium iodide (PI) (Biolegend) were performed by using flow cytometry.

Enzyme-linked immunosorbent assay (ELISA)

Raw 264.7 cells were seeded onto a 24-well plate (1.5×10^5 cells per 500 µL). The cells were pretreated with HBM-derived exosomes in dose-dependent manners (250, 500, 1000 µg/mL) for 24 h and stimulated by LPS (1 µg/mL; Sigma-Aldrich) for 18 h. Then, supernatants of each wells were harvested to determine inflammatory cytokines, such as IL-1β, IL-6, TNF-α, and prostaglandin E2 (PGE_2). The protein levels of cytokines were measured by the manual method of sandwich ELISA. In brief, purified Armenian hamster anti-mouse/rat IL-1β antibody (3 µg/mL, clone B122; eBioscience), purified rat anti-mouse IL-6 antibody (3 µg/mL, clone MP5-20F3; BD Biosciences), and purified Armenian hamster anti-mouse/rat TNF-α antibody (2 µg/mL, clone TN3-19.12; eBioscience) were coated on 96-well immunoplate at 4 °C for overnight (O/N). The plate was washed with 0.05% (v/v) Tween 20 (VWR, Radnor, PA, USA) in PBS (0.05% PBST) and blocked with 3% (w/v) BSA (MP Biomedicals, Irvine, CA, USA) in PBS at RT for 2 h. Then, the supernatants were added to each wells for again O/N. Biotinylated rabbit anti-mouse IL-1β antibody (4 µg/mL, clone polyclonal; eBioscience), biotinylated rat anti-mouse IL-6 antibody (2 µg/mL, clone MP5-32C11; BD Biosciences), and biotinylated rabbit anti-mouse/rat TNF-α antibody (2 µg/mL, clone polyclonal; eBioscience) were incubated in the plate at RT for 30 min, and alkaline phosphatase-conjugated streptavidin (Jackson ImmunoResearch, West Grove, PA, USA) was added to the plate at RT for 20 min. 4-nitrophenyl phosphate disodium salt hexahydrate (20 mg/mL, Sigma-Aldrich) was then treated, and the optical density (OD) was measured by an EMax microplate reader at 405 nm. Standard curves for the quantification of cytokine levels were demonstrated using recombinant murine IL-1β, IL-6, and TNF-α (Peprotech, Rocky Hill, NJ, USA). The secretion of PGE_2 by LPS-stimulated RAW 264.7 cells was identified using a PGE_2 ELISA kit (Cayman Chemical, Ann Arbor, MI, USA) following the manufacturer's instructions.

Nitric oxide (NO) assay

Raw 264.7 cells were seeded onto 24-well plate (1.5×10^5 cells per 500 µL), and pretreated with 250–1000 µg/mL of HBM-derived exosome for 24 h. Then, 1 µg/mL of LPS (Sigma-Aldrich) was used for stimulation of the cells. The supernatant was harvested and 50 µL of Griess reagent (Sigma-Aldrich) was added to the 50 µL of supernatant in 96-well plate. The OD was determined by an EMax microplate reader at 540 nm. Sodium nitrite (Junsei Chemical Co., Ltd., Chuo-ku, Tokyo, Japan) was used to construct a nitrite standard curve (0–100 µM) for the calculation of NO production level.

Immunoblotting

The samples were lysed and proteins were extracted by Pierce™ RIPA Buffer (Thermo-Fisher Scientific, Rockford, IL, USA). The Protein concentration was identified and synchronized by using a Pierce™ BCA Protein Assay Kit (Thermo-Fisher Scientific). The samples were resuspended in 5× Protein Sample Buffer (0.5 M Tis-HCl, 20% (v/v) glycerol, 20% (v/v) of 10% (w/v) SDS, 5% (w/v) bromophenol blue) containing 5% (v/v) 2-mercaptoethanol and boiled 95 °C for 5 min. Samples were resolved by SDS-PAGE using 10%, 12%, and 15% gels depending on protein size. SDS-

PAGE was performed at a constant voltage of 100 V, and proteins were transferred to a polyvinylidene fluoride membrane (Amersham, Piscataway, NJ, USA). The membranes with protein were blocked for 2 h at RT with blocking solution (5% (w/v) of skim milk with 0.1% PBST). Blocked membranes were then incubated with rabbit monoclonal anti-CD81, CD9, HSP70, Annexin V, CD54/ICAM-1, Flotillin-1, Alix, GM130 antibodies (1:1000; Cell signaling Technology, Danvers, MA, USA), rabbit polyclonal anti- inducible nitric oxide synthase (iNOS), cyclooxygenase-2 (COX-2) (1:1000, Santa Cruz Biotechnology, Dallas, TX, USA) antibodies, mouse monoclonal anti-ERK, JNK (1:1000; Santa Cruz Biotechnology) antibodies, rabbit monoclonal anti-p-ERK, p-JNK (1:1000; Cell signaling Technology) antibodies, rabbit monoclonal anti-STAT1, STAT3, STAT5, STAT6, p-STAT1, p-STAT3, p-STAT5, p-STAT6 (1:1000, Cell signaling Technology), rabbit polyclonal anti-ZO-1, OCLN, CLDN3 (1:1000, Invitrogen), and mouse monoclonal anti-GAPDH antibody (1:200; Santa Cruz Biotechnology) with shaking for overnight at 4 °C. Membranes were then incubated with horseradish peroxidase (HRP)-conjugated goat anti-rabbit IgG (Bio-Rad Laboratories, Hercules, CA, USA) and goat anti-mouse IgG (cell signaling Technology) diluted 1:2000 for 2 h at RT. Finally, the signals were visualized by the Westsave Femto™ detection kit (Abfrontier, Seoul, Korea) and quantified using Fusion Solo X (Vilver, Paris, France).

Differentiation of naïve CD4$^+$ T cells

The naïve CD4$^+$ T cells were seeded on a 24-well plate at a density of 4×10^5 cells per 500 μL for each well. The cells were simultaneously stimulated and treated by cytokines that differentiated into different subsets of CD4$^+$ T cell and HBM-derived exosome in a dose-dependent manner, respectively. Regulatory T cell (Treg cell) was differentiated by stimulation of plate-bound anti-mouse CD3e (1 μg/mL; clone 145-2C11, eBioscience) and anti-mouse CD28 (1 μg/mL; clone 37.51, eBioscience) antibodies, and adding IL-2 (10 ng/mL, BD Biosciences) and TGF-β1 (2.5 ng/mL, BD Biosciences). Th17 cell was differentiated by stimulation of plate-bound anti-mouse CD3e (1 μg/mL; clone 145-2C11, eBioscience) and anti-mouse CD28 (1 μg/mL; clone 37.51, eBioscience) antibodies, and adding IL-6 (25 ng/mL, BD Biosciences) and TGF-β1 (2.5 ng/mL, BD Biosciences). Th1 cell was differentiated by stimulation of plate-bound anti-mouse CD3e (5 μg/mL; clone 145-2C11, eBioscience) and anti-mouse CD28 (2 μg/mL; clone 37.51, eBioscience) antibodies, and adding IL-2 (20 ng/mL, BD Biosciences) and IL-12 (20 ng/mL, BD Biosciences). Th2 cell was differentiated by stimulation of plate-bound anti-mouse CD3e (5 μg/mL; clone 145-2C11, eBioscience) and soluble anti-mouse CD28 (2 μg/mL; clone 37.51, eBioscience) antibodies, and adding IL-2 (20 ng/mL, BD Biosciences) and IL-4 (100 ng/mL, BD Biosciences).

Re-epithelization assay

Caco-2 cells were seeded at a density of 3×10^4 cells per well onto Culture-Insert 2 Well devices (Ibidi, Gräfelfing, Germany), which were placed in a 24-well plate. A total of 70 μL of cell suspension was added to each well and incubated at 37 °C with 5% CO_2 until the cells reached 95% confluence. The Culture-Insert 2 Well was then carefully removed, and 500 μL of media was added. Following this, HBM-derived exosomes were administered in a dose-dependent manner (250, 500, and 1000 μg/mL). The extent of cell migration, represented by the percentage of re-epithelialization, was monitored using the JuLi Stage Real-Time Cell History Recorder (NanoEnTek, Inc., Seoul, Korea).

Mouse

Male C57BL/6 mice aged 4 to 5 weeks were acquired from Raonbio (Korea). These mice were housed under specific pathogen-free conditions, with air conditioning and a 12-h light/dark cycle. Prior to the establishment of the DSS-induced colitis model, mice were subjected to a one-week acclimatization period. During this time, they were housed in groups of 3–4 per cage and provided unrestricted access to food and water. To ensure unbiased group allocation, the random assignment of cages to experimental groups was conducted by a researcher not directly involved in the experiments. To minimize potential confounders, treatments were randomized and measurements were conducted in a blind manner. Animal cages were regularly rotated within the housing unit to account for any location-based effects. All experimental procedures (oral administration and sacrifice) were approved by the Institutional Animal Care and Use Committee at Chung-Ang University reviewed and approved this study (Ethics Approval Number. 202301020031). For the mouse sacrifice, euthanasia was performed by CO_2 inhalation in accordance with the guidelines of the Institutional Animal Care and Use Committee at Chung-Ang University. Based on recent studies, it was determined that examining a moderate dose rather than a high dose of exosomes would be more effective in the acute colitis model[58]. According to previous studies, for the HBM-derived exosomes-administered group, mice were orally given exosomes in PBS (100 μL) daily through the GI tract at a dose of 3 mg•kg•bw^{-1}•day^{-1}, starting 1 week before inducing colitis and continuing until the day of sacrifice. While administering HBM-derived exosomes, the acute colitis mice models were allowed free access to DSS-containing water for 5 days, followed by a 2-day rest period before sacrifice. In the chronic colitis mouse model, according to a previous study, mice were given DSS-containing water ad libitum for 5 days, followed by a 9-day rest period, and this cycle was repeated three times[59,60]. No inclusion or exclusion criteria were established for animals, experimental units, or data points in this study. All collected data were included in the analysis. In addition, no animals, experimental units, or data points were excluded from the analysis in any of the experimental groups.

Establishment of DSS-induced colitis models and cell preparation

Two types of colitis mouse models were induced by DSS: acute and chronic colitis mouse models. The experiments were conducted using these two models, and the at least 6-week male mice were divided into three groups: the control group ($n = 10$), the DSS-treated group ($n = 10$), and the DSS + HBM-derived exosome-treated group ($n = 10$). Each model was replicated twice. The body weight and disease activity index (DAI) scores were monitored and recorded daily to evaluate the clinical efficacy of the exosomes. The DAI score was measured based on standard indicators (Supplementary Table 1). Immune cells were isolated from the spleen, mesenteric lymph node (MLN), and colon using different procedures. For the spleen and MLN, cells were harvested by homogenizing the tissues after adding 1 ml of ACK lysis buffer. To neutralize the ACK reaction, 3 ml of RPMI media with 10% FBS was added. The resulting suspension was filtered through a 70 μm mesh to separate cells and then centrifuged for 5 min at 1300 rpm. This process successfully isolated immune cells from the spleen and MLN. In contrast, the isolation of colonic immune cells involved a different method. First, fat was removed from the colon, which was then washed with PBS from both ends using a blunt-end gavage needle. The colon was inverted onto a polyethylene tube (2.42 mm) to expose the mucosa. It was washed three times with 8 ml of calcium and magnesium-free PBS for 2 min at RT, followed by shaking for 10 min with 1 mM DTT/PBS by hand. The colon was then incubated three times for 8 min with 30 mM EDTA/PBS at RT, with manual shaking in between. Afterward, the colon was washed with PBS for 2 min at RT and shaken carefully to avoid eluting villi. The tissue was digested with 10 ml of collagenase solution in a 15 ml conical tube for 90 min at 37 °C. After digestion, the colon was gently shaken for 12 min. The supernatants containing eluted cells were passed through a 70-μm cell strainer, followed by centrifugation for 6 min at 1800 rpm at RT. Finally, immune cells were isolated using the Percoll gradient method with 44% (v/v) and 66% (v/v) solutions.

Histology and immunohistochemistry (IHC)

The colon samples were prepared using the "Swiss roll" method, involving longitudinal-transverse sections. For histological examination, the colon was formalin-fixed and paraffin-embedded, then sectioned at 5 μm and placed on adhesion slides (Epredia, Marlborough, MA, USA). The sections were stained with hematoxylin and eosin (H&E, Sigma-Aldrich) and mounted using DPX Mountant (Sigma-Aldrich) to enhance visualization of

inflammation and pathological changes in the colon. Immunohistochemistry (IHC) assays were performed on the sections by first de-paraffinizing them using xylene (Sigma-Aldrich) and then rehydrating them through a graded series of alcohols to water. Epitope retrieval was carried out using a retrieval solution (Dako, Nowy Sącz, Poland). Endogenous peroxidase activity was inhibited by incubating the slides in 3% H_2O_2 (Sigma-Aldrich) for 10 min at RT. The sections were blocked using goat serum (Vector Laboratories, Newark, CA, USA) and incubated overnight with anti-mouse F4/80 (1:200, Cell Signaling Technology) or anti-mouse CD3e (1:200, Cell Signaling Technology) at RT in a humidified chamber. After washing the sections with 0.1% PBST, they were incubated for one hour at RT with biotinylated anti-mouse secondary antibodies (Vector Laboratories) and rinsed again in 0.1% PBST. The tissue was then treated with avidin-biotin-peroxidase complexes for one hour at RT, following the manufacturer's guidelines (VECTASTAIN® Elite® ABC-HRP Kit, Vector Laboratories). Finally, the sections were developed using Vector® DAB Peroxidase Substrate (Vector Laboratories), counterstained with Hematoxylin (Abcam, Cambridge, UK), and cover-slipped with DPX Mountant (Sigma-Aldrich).

Flow cytometry

Flow cytometry was also performed to identify the subsets of $CD4^+$ T cells and the phenotypes of immune cells which were isolated in the spleen and MLN, and colon. To observe the TNF-α and TGF-β-producing macrophages, regulatory T cells, Th17 cells, Th1 cells, and Th2 cells, the immune cells were re-stimulated by PMA, ionomycin, and golgi stop (ebioscience).Then, the cells were stained with many types of antibodies, such as FITC anti-mouse/human CD11b antibody (clone:M1/70, Biolegend), Alexa Fluor 488 anti-mouse CD86 antibody (clone: GL-1, Biolegend), PE anti-mouse CD3e antibody (clone:17 A2, Biolegend), PE anti-mouse CD206 (MMR) recombinant antibody (clone:QA17A35, Biolegend), PE anti-mouse CD25 antibody (clone:PC61, Biolegend), PE anti-mouse IL-17A antibody (clone:TC11-18H10.1, Biolegend), PE anti-mouse t-bet antibody (clone:4B10, ebioscience), PE anti-GATA3 antibody (clone:16E10A23, Biolegend), PerCP anti-mouse CD8a antibody (clone:53-6.7, Biolegend), PerCP/Cyanine5.5 anti-mouse LAP(TGF-β1) antibody (clone:TW7-16B4, Biolegend), PerCP/Cyanine5.5 anti-mouse Foxp3 antibody (clone:FJK-16s, ebioscience), PerCP/Cy5.5 anti-mouse RORγt antibody (clone:Q31-378, Biolegend), PE/cyanine7 anti-mouse IFN-γ antibody (clone: XMG1.2, Biolegned), PE/Cyanine7 anti-mouse IL-4 antibody (clone:11B11, Biolegned), APC anti-mouse CD4 antibody (clone: RM4-5, Biolegend), and APC anti-mouse TNF-α antibody (clone: RM4-5, Biolegend). The Total macrophages ($CD11b^+CD3e^-CD4^-CD8^-$ cells), Total T cells ($CD11b^-CD4^+$ cells), $CD4^+$ T cells ($CD11b^-CD3e^+CD8^-CD4^+$ cells), $CD8^+$ T cells ($CD11b^-CD3e^+CD4^-CD8^+$ cells), TNF-α-producing macrophages ($CD86^+TNF\text{-}\alpha^+$ cells), TGF-β-producing macrophages ($CD206^+TGF\text{-}\beta^+$ cells), Treg cells ($CD25^+Foxp3^{GFP+}IL\text{-}10^+CD4^+$ and $CD25^+Foxp3^+CD4^+$ cells), Th17 cells ($IL\text{-}17a^+$ $ROR\gamma t^+CD4^+$ cells), Th1 cells ($t\text{-}bet^+$ $IFN\text{-}\gamma^+CD4^+$ cells), and Th2 cells ($GATA3^+IL\text{-}4^+CD4^+$ cells) were detected by FACS Calibur (BD Biosciences, Franklin Lakes, NJ, USA) and CellQuestPro software was used to analyze.

Statistical analysis

At least three replicates of the experiment were conducted, and numerical data were determined as the average ± SEM by GraghPad Prism v. 5 software (GraghPad, San Diego, CA, USA). The significance of the data were examined by one-way ANOVA with Tukey's post hoc test. $^*p < 0.05$; $^{**}p < 0.01$, $^{***}p < 0.001$.

Data availability

The data supporting this article's findings are available from the corresponding author upon reasonable request.

Received: 26 February 2024; Accepted: 27 February 2025;
Published online: 20 March 2025

References

1. Kim, K. U., Kim, W. H., Jeong, C. H., Yi, D. Y. & Min, H. More than nutrition: therapeutic potential of breast milk-derived exosomes in cancer. *Int. J. Mol. Sci.* **21**, 7327 (2020).
2. Nutrition, E. C. et al. Breast-feeding: a commentary by the ESPGHAN committee on nutrition. *J. Pediatr. Gastroenterol. Nutr.* **49**, 112–125 (2009).
3. Ip, S. et al. Breastfeeding and maternal and infant health outcomes in developed countries. *Evid. Rep. Technol. Assess*. 1–186 (2007).
4. Yu, J. C. et al. Innate immunity of neonates and infants. *Front. Immunol.* **9**, 1759 (2018).
5. Lasser, C. et al. Human saliva, plasma and breast milk exosomes contain RNA: uptake by macrophages. *J. Transl. Med.* **9**, 9 (2011).
6. Ren, S. et al. Microvesicles from human adipose stem cells promote wound healing by optimizing cellular functions via AKT and ERK signaling pathways. *Stem Cell Res. Ther.* **10**, 47 (2019).
7. Zhang, S. et al. MSC exosomes mediate cartilage repair by enhancing proliferation, attenuating apoptosis and modulating immune reactivity. *Biomaterials* **156**, 16–27 (2018).
8. Segura, E. et al. ICAM-1 on exosomes from mature dendritic cells is critical for efficient naive T-cell priming. *Blood* **106**, 216–223 (2005).
9. Wang, Y. et al. MiR-548a-3p regulates inflammatory response via TLR4/NF-kappaB signaling pathway in rheumatoid arthritis. *J. Cell Biochem.* **120**, 1133–1140 (2019).
10. Tkach, M. et al. Qualitative differences in T-cell activation by dendritic cell-derived extracellular vesicle subtypes. *EMBO J.* **36**, 3012–3028 (2017).
11. Yanez-Mo, M. et al. Biological properties of extracellular vesicles and their physiological functions. *J. Extracell. Vesicles* **4**, 27066 (2015).
12. Robbins, P. D. & Morelli, A. E. Regulation of immune responses by extracellular vesicles. *Nat. Rev. Immunol.* **14**, 195–208 (2014).
13. Admyre, C. et al. Exosomes with immune modulatory features are present in human breast milk. *J. Immunol.* **179**, 1969–1978 (2007).
14. Herwijnen, M. J. C. et al. Abundantly present miRNAs in milk-derived extracellular vesicles are conserved between mammals. *Front. Nutr.* **5**, 81 (2018).
15. Ballard, O. & Morrow, A. L. Human milk composition: nutrients and bioactive factors. *Pediatr. Clin. North Am.* **60**, 49–74 (2013).
16. Hock, A. et al. Breast milk-derived exosomes promote intestinal epithelial cell growth. *J. Pediatr. Surg.* **52**, 755–759 (2017).
17. Roda, G. et al. Crohn's disease. *Nat. Rev. Dis. Primers* **6**, 22 (2020).
18. Kobayashi, T. et al. Ulcerative colitis. *Nat. Rev. Dis. Primers* **6**, 74 (2020).
19. Sartor, R. B. Mechanisms of disease: pathogenesis of Crohn's disease and ulcerative colitis. *Nat. Clin. Pract. Gastroenterol. Hepatol.* **3**, 390–407 (2006).
20. Sartor, R. B. Microbial influences in inflammatory bowel diseases. *Gastroenterology* **134**, 577–594 (2008).
21. Bosca-Watts, M. M. et al. Pathogenesis of Crohn's disease: bug or no bug. *World J. Gastrointest. Pathophysiol.* **6**, 1–12 (2015).
22. Caenepeel, C., Sadat Seyed Tabib, N., Vieira-Silva, S. & Vermeire, S. Review article: how the intestinal microbiota may reflect disease activity and influence therapeutic outcome in inflammatory bowel disease. *Aliment. Pharmacol. Ther.* **52**, 1453–1468 (2020).
23. He, S., Liu, G. & Zhu, X. Human breast milk-derived exosomes may help maintain intestinal epithelial barrier integrity. *Pediatr. Res.* **90**, 366–372 (2021).
24. Martin, C. et al. Human breast milk-derived exosomes attenuate cell death in intestinal epithelial cells. *Innate Immun.* **24**, 278–284 (2018).
25. Miyake, H. et al. Human breast milk exosomes attenuate intestinal damage. *Pediatr. Surg. Int.* **36**, 155–163 (2020).
26. van Herwijnen, M. J. et al. Comprehensive proteomic analysis of human milk-derived extracellular vesicles unveils a novel functional proteome distinct from other milk components. *Mol. Cell Proteomics* **15**, 3412–3423 (2016).

27. Naslund, T. I. et al. Exosomes from breast milk inhibit HIV-1 infection of dendritic cells and subsequent viral transfer to CD4+ T cells. *AIDS* **28**, 171–180 (2014).
28. Torregrosa Paredes, P. et al. Differences in exosome populations in human breast milk in relation to allergic sensitization and lifestyle. *Allergy* **69**, 463–471 (2014).
29. Zempleni, J. et al. Biological activities of extracellular vesicles and their cargos from bovine and human milk in humans and implications for infants. *J. Nutr.* **147**, 3–10 (2017).
30. Galley, J. D. & Besner, G. E. The therapeutic potential of breast milk-derived extracellular vesicles. *Nutrients* **12**, 745 (2020).
31. Zhang, Q., Jeppesen, D. K., Higginbotham, J. N., Franklin, J. L. & Coffey, R. J. Comprehensive isolation of extracellular vesicles and nanoparticles. *Nat. Protoc.* **18**, 1462–1487 (2023).
32. Noguchi, S. et al. BeWo exomeres are enriched for bioactive extracellular placenta-specific C19MC miRNAs. *J. Reprod. Immunol.* **161**, 104187 (2024).
33. Benmoussa, A. et al. Concentrates of two subsets of extracellular vesicles from cow's milk modulate symptoms and inflammation in experimental colitis. *Sci. Rep.* **9**, 14661 (2019).
34. Reif, S. et al. Cow and human milk-derived exosomes ameliorate colitis in DSS murine model. *Nutrients* **12**, 2589 (2020).
35. Liu, T., Zhang, L., Joo, D. & Sun, S. C. NF-kappaB signaling in inflammation. *Signal Transduct. Target Ther.* **2**, 17023 (2017).
36. Kaminska, B. MAPK signalling pathways as molecular targets for anti-inflammatory therapy-from molecular mechanisms to therapeutic benefits. *Biochim. Biophys. Acta* **1754**, 253–262 (2005).
37. Xie, M. Y. et al. Porcine milk exosome MiRNAs attenuate LPS-induced apoptosis through inhibiting TLR4/NF-κB and p53 pathways in intestinal epithelial cells. *J. Agric. Food Chem.* **67**, 9477–9491 (2019).
38. Arntz, O. J. et al. Oral administration of bovine milk derived extracellular vesicles attenuates arthritis in two mouse models. *Mol. Nutr. Food Res.* **59**, 1701–1712 (2015).
39. Villarino, A. V. Transcriptional programing of T cell metabolism by STAT family transcription factors. *Eur. J. Immunol*. **53**, e2048825 (2023).
40. Takeda, K. et al. Essential role of Stat6 in IL-4 signalling. *Nature* **380**, 627–630 (1996).
41. Hu, X. & Ivashkiv, L. B. Cross-regulation of signaling pathways by interferon-gamma: implications for immune responses and autoimmune diseases. *Immunity* **31**, 539–550 (2009).
42. Yuan, S. et al. Interleukin-17 stimulates STAT3-mediated endothelial cell activation for neutrophil recruitment. *Cell Physiol. Biochem.* **36**, 2340–2356 (2015).
43. Di, S. J., Cui, X. W., Liu, T. J. & Shi, Y. Y. Therapeutic potential of human breast milk-derived exosomes in necrotizing enterocolitis. *Mol. Med.* **30**, 243 (2024).
44. Celik, E. et al. Human breast milk exosomes: affecting factors, their possible health outcomes, and future directions in dietetics. *Nutrients* **16**, 3519 https://doi.org/10.3390/nu16203519 (2024).
45. Chiba, T. & Maeda, T. Human milk exosomes induce ZO-1 expression via inhibition of REDD1 expression in human intestinal epithelial cells. *Biol. Pharm. Bull.* **46**, 893–897 (2023).
46. Tong, L. et al. Milk-derived extracellular vesicles protect intestinal barrier integrity in the gut-liver axis. *Sci. Adv.* **9**, eade5041 (2023).
47. Cummings, R. J. et al. Different tissue phagocytes sample apoptotic cells to direct distinct homeostasis programs. *Nature* **539**, 565–569 (2016).
48. Xue, G., Hua, L., Zhou, N. & Li, J. Characteristics of immune cell infiltration and associated diagnostic biomarkers in ulcerative colitis: results from bioinformatics analysis. *Bioengineered* **12**, 252–265 (2021).
49. Zhao, J. et al. Th17 cells in inflammatory bowel disease: cytokines, plasticity, and therapies. *J. Immunol. Res.* **2021**, 8816041 (2021).
50. Brand, S. Crohn's disease: Th1, Th17 or both? The change of a paradigm: new immunological and genetic insights implicate Th17 cells in the pathogenesis of Crohn's disease. *Gut* **58**, 1152–1167 (2009).
51. Jacobse, J., Li, J., Rings, E., Samsom, J. N. & Goettel, J. A. Intestinal regulatory T cells as specialized tissue-restricted immune cells in intestinal immune homeostasis and disease. *Front. Immunol.* **12**, 716499 (2021).
52. Bamias, G. & Cominelli, F. Role of Th2 immunity in intestinal inflammation. *Curr Opin Gastroenterol*. **31**, 471 (2015).
53. Golan, Y. & Assaraf, Y. G. Genetic and physiological factors affecting human milk production and composition. *Nutrients* **12**, 1500 (2020).
54. Lokossou, G. A. G., Kouakanou, L., Schumacher, A. & Zenclussen, A. C. Human breast milk: from food to active immune response with disease protection in infants and mothers. *Front. Immunol.* **13**, 849012 (2022).
55. Thery, C., Zitvogel, L. & Amigorena, S. Exosomes: composition, biogenesis and function. *Nat. Rev. Immunol.* **2**, 569–579 (2002).
56. Miklavcic, J. J., Paterson, N., Hahn-Holbrook, J. & Glynn, L. Impact of FADS genotype on polyunsaturated fatty acid content in human milk extracellular vesicles: a genetic association study. *JPEN J. Parenter. Enteral. Nutr.* **48**, 479–485 (2024).
57. Yi, D. Y. & Kim, S. Y. Human breast milk composition and function in human health: from nutritional components to microbiome and microRNAs. *Nutrients* **13**, 3094 (2021).
58. Tong, L. et al. Milk-derived extracellular vesicles alleviate ulcerative colitis by regulating the gut immunity and reshaping the gut microbiota. *Theranostics* **11**, 8570–8586 (2021).
59. Hoffmann, M. et al. A refined and translationally relevant model of chronic DSS colitis in BALB/c mice. *Lab Anim.* **52**, 240–252 (2018).
60. Okayasu, I. et al. A novel method in the induction of reliable experimental acute and chronic ulcerative colitis in mice. *Gastroenterology* **98**, 694–702 (1990).

Acknowledgements

This research was supported by the National Research Foundation of Korea (NRF) grant funded by the Korean government (Ministry of Science and ICT), grant number NRF-2021R1F1A1061287 (H.M.) and Basic Science Research Program through the National Research Foundation of Korea (NRF) funded by the Ministry of Education, grant number NRF-2021R1A6A3A13045991 (K.-U.K.).

Author contributions

K.-U.K.: Investigation, funding acquisition, methodology, formal analysis, and writing-original draft; J.K., H.J., K.B.D., and B.K.K.: Methodology and validation; Y.W.J.: Methodology; D.Y.Y.: Conceptualization, resources, and writing-review & editing; H.M.: Conceptualization, funding acquisition, investigation, and writing-review & editing. All authors have read and agreed to the published version of the manuscript.

Competing interests

The authors have declared that no conflict of interest exists.

Additional information

Supplementary information The online version contains supplementary material available at https://doi.org/10.1038/s41538-025-00400-3.

Correspondence and requests for materials should be addressed to Hyeyoung Min.